

COUPLER MATCHING TECHNIQUES FOR C-BAND ACCELERATING SECTION

K. Yokoyama, T. Kamitani, T. Sugimura, S. Ohsawa, K. Kakihara, M. Ikeda, Accelerator Laboratory,
T. Takatomi, Mechanical Engineering Center,
KEK, 1-1 Oho, Tsukuba, Ibaraki 305-0801, Japan

Abstract

Research and development of the C-band accelerating section has been in progress at KEK since 2002 [1]. This paper reports on the development of the second prototype accelerating section. Both input/output couplers have a single port and their cells are the same length as the waveguide width. The coupler irises are thicker than the first prototype for preventing the rf breakdown at the iris edge. The coupler cavity diameters and the coupling irises were optimized by using the iteration of the rf measurement which is based on the nodal shift method. The high-power test of the accelerating section at the test stand has been performed for a month. Rf breakdown frequency has been reduced.

INTRODUCTION

An acceleration field gradient of at least 42 MV/m is required for the superKEKB injector linac where S-band modules in part of the present linac are replaced by C-band modules. The first prototype has been operated in the present linac, however the rf breakdown problem occurred initially, it has been achieved approximately 42 MV/m at present. The design of the first prototype is based on half-scale of the present S-band section. Almost every rf breakdown events occurred around the input coupler, so the thin iris edge of the coupler could have been caused the rf breakdown problem [2]. Other designs have been approached to reduce the problem [3].

DESIGN AND FABRICATION

Specifications of the C-band section are shown in Table 1. The structure is a disk-loaded waveguide with a 120 degree phase advance per cell which yields a quasi-constant gradient. Figure 1 shows the coupler designs of the first prototype (CKM001) and the second prototype (CKK001). The CKK001's iris with a 4 mm thick is thicker than CKM001's one to suppress the rf breakdown. The coupler uses a single port and the coupler cell is the same length as the waveguide width (WR-187). This means the coupler cavity and the regular cell have a different length along the beam axis. So that indicates a phase advance of the coupler cavity is not the same as that of the regular cells unlike with CKM001. A different tuning method from the kyhl method should be considered. The schematic of CKK001 is shown in Fig. 2. A coupler and attachments for an rf measurement are brazed with gold before optimizing its size. Couplers and regular cells are united by copper electroforming and accessories such as a water jacket and flanges are TIG

welded. Finally, plungers are joined by welding after optimizing the corner radius of the beam-hole.

Table 1: Specifications of the C-band section

operation frequency	5712.000	MHz
operation temperature	30.0	degC
number of cells.	54 regular cells + 2 couplers	
section length	926.225 (55 cells) mm	
phase advance per cell	$2\pi/3$ -mode	
cell length	17.495	mm
disk thickness (t)	2.500	mm
iris diameter (2a)	12.475 ~ 10.450	mm
cavity diameter (2b)	41.494 ~ 41.010	mm
shunt impedance (r_0)	74.6 ~ 85.1	M Ω /m
Q factor	9703 ~ 9676	
group velocity (v_g/c)	1.9 ~ 1.0	%
filling time	~ 240	ns
attenuation parameter (τ)	~ 0.44	

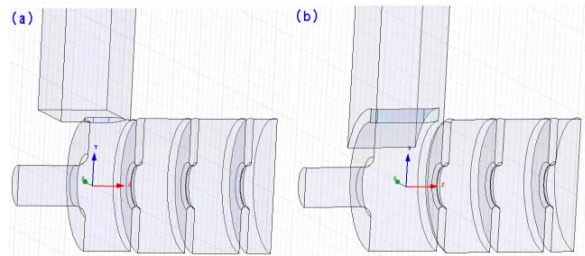


Figure 1: Coupler designs of (a) the first prototype (CKM001) and (b) the second prototype (CKK001).

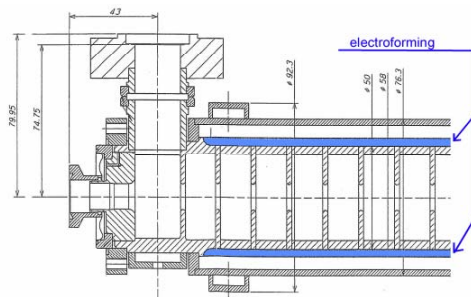


Figure 2: Schematic of the second prototype of C-band section.

MATCHING TECHNIQUES

A coupler dimension was extracted from simulation of a scattering matrix element S_{11} by using MAFIA-T3TM and HFSSTM. The cavity diameter $2b_c$ and the iris width W were manufactured undersize because the results of the simulation could have a certain error. Three couplers each for the input and the output were prepared to optimize the dimension. Figure 3 shows couplers, beam-holes and a setup for rf measurements. A coupler, a plunger with a

beam-hole and 6 cells are put together by jigs. $2b_c$ and W were processed until a phase advance was measured such as fig. 4 (a). Measuring the resonance frequency f_{res} in a coupler cavity was reliable for this procedure at first. The target frequency was the average value between the resonant frequency for the $\pi/2$ mode and the $2\pi/3$ mode since it's the basic approach to the matching procedure as the kyhl method [4]. As shown in (b), a 120 degree phase advance per cell wasn't obtained under this procedure as was expected. Therefore, the following method of optimizing the coupler dimension was contrived for accomplishing coupler tuning.

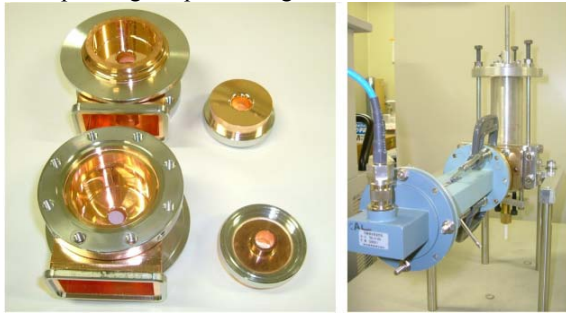


Figure 3: Couplers, beam-holes and setup for low-power experiments.

Method of optimizing

The appropriate size of W is a concern to obtain the proper coupling. There's a simple method to see if $2b_c$ is undersize or oversize corresponding to the size of W . The resonant frequency lowers when a piece of Teflon is inserted in the cavity. On the other hand, the resonance frequency rises when the corner radius of the beam-hole is enlarged. These procedures have the same effects of changing the size of $2b_c$. The diameter of the first cell $2b_1$ was also modified to obtain the proper coupling in the practical procedure. To estimate the amount of modification, each phase deviation from a 120 degree phase advance could be approximated as the first order expansion by

$$\begin{pmatrix} \Delta\theta_1 \\ \Delta\theta_2 \\ \Delta\theta_3 \end{pmatrix} = \begin{pmatrix} \frac{\partial\theta_1}{\partial(2b_c)} & \frac{\partial\theta_1}{\partial(2b_1)} & \frac{\partial\theta_1}{\partial(W)} \\ \frac{\partial\theta_2}{\partial(2b_c)} & \frac{\partial\theta_2}{\partial(2b_1)} & \frac{\partial\theta_2}{\partial(W)} \\ \frac{\partial\theta_3}{\partial(2b_c)} & \frac{\partial\theta_3}{\partial(2b_1)} & \frac{\partial\theta_3}{\partial(W)} \end{pmatrix} \begin{pmatrix} \Delta 2b_c \\ \Delta 2b_1 \\ \Delta W \end{pmatrix} \quad (1),$$

where, θ_1 , θ_2 and θ_3 represent the deviation of a phase advance between each cell, and $\Delta\theta_1$, $\Delta\theta_2$ and $\Delta\theta_3$ represent the each deviation from a 120 degree phase advance and $\Delta 2b_c$, $\Delta 2b_1$ and ΔW represent the amount of modification, respectively. The sum of θ_1 , θ_2 and θ_3 is 360 degree and the each deviation is 120 degree ideally. But solving Eq. (1) directly is not practical to find a solution because the measuring and processing accuracy have an error slightly. Thus, only two deviations were adopted for estimating. Figure 4 show the results of the nodal shift, Table 2 shows the coupler dimension corresponding to fig. 4 and Table 3 shows an example of the matrix elements which were obtained from measuring and processing,

respectively. Figure 5 shows the history of the dimension of input/output couplers. Figure 4 (c) shows the results of the nodal shift after accomplishing coupler tuning; this is sufficient to a 120 degree phase advance per cell. After coupler tuning with 6 cells, the inner diameter of regular cell's spacers were processed. The amount of modification was determined by measuring the nodal shift as well. Figure 4 (d) shows the results of the nodal shift after optimizing spacers of all regular cells. A 120 degree phase advance per cell at the target frequency was obtained. In general, a resonance frequency shift is caused in electroforming process because regular cells could be pressured by a stress and the coupler dimension could be shrunk. The resonance frequency shift was estimated by the result of electroforming a test-section which had 6 cells. The target frequency contained this estimation.

Manufacturing process

The value of VSWR is also our concern in manufacturing an accelerating section. A voltage standing-wave ratio (VSWR) of less than 1.4 is required. There's a possibility VSWR will change in a welding process because of a thermal stress. VSWR and the surface temperature of couplers were measured every time TIG welding was executed. Figure 6 shows the measurement results of VSWR vs. frequency before and after cooper electroforming. The frequency of the minimum VSWR was shifted in large quantities from this result. The pressure induced by sticking couplers and regular cells could have caused a certain strain of the couplers. The optimization of the corner radius of beam-holes was implemented to compensate for the frequency shift before welding. The shift was improved (see fig. 7). The VSWR vs. frequency was also changed during welding accessories. The corner radius of beam-holes was modified as well and the plungers were welded. The final result of VSWR vs. frequency is shown in fig. 7. The VSWR at the target frequency is adequately low but the bandwidth turned out to be narrow.

HIGH-POWER TEST

CKK001 was installed in a high-power test stand for rf aging. A 5-stub tuner was used to expand the bandwidth of the accelerating section. Figure 8 shows the measurement results of VSWR vs. frequency before and after adjusting the 5-stub tuner. The bandwidth is improved and the VSWR of 1.13 at the target frequency in the atmosphere is obtained. Rf aging has been performed for about a month ($\sim 1.1 \times 10^8$ shots). The rf power of about 40 MW with a pulse width of 500 ns and a pulse repetition rate of 50 Hz has been fed to CKK001. The number of rf breakdown events is several times per day. This performance is satisfactory for using as a practical c-band accelerating section.

CONCLUSION

The method of a coupler tuning was achieved by taking advantage of a piece of Teflon and beam-holes with a

different corner radius, which have the same effects of changing the size of $2b_c$, and the nodal shift method. CKK001 has shown a good performance with no rf breakdown problem. It will be installed in this summer for beam acceleration tests.

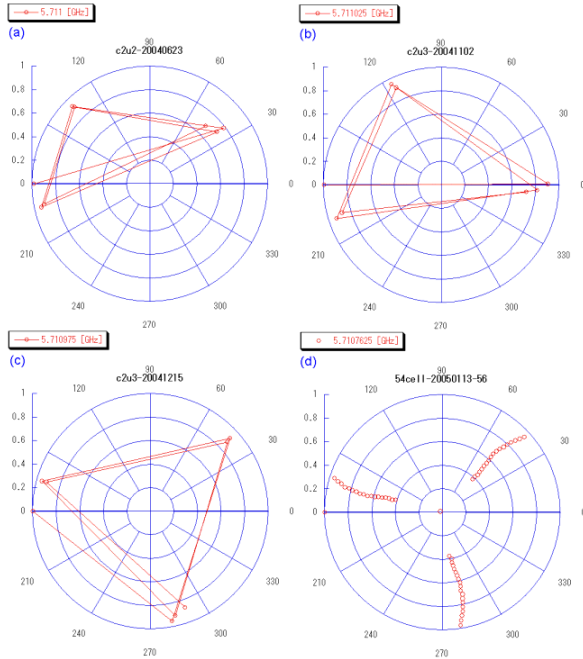


Figure 4: The results of the nodal shift. (a) and (b) are of the procedure for homing in on f_{res} , (c) is of after accomplishing tuning, (d) is of with regular cells.

Table 2: The coupler dimension corresponding to fig. 4

	$2b_c$ [mm]	W [mm]	$2b_1$ [mm]	f_{res} [GHz]
(a)	40.23	16.104	41.49	5.711000
(b)	40.31	16.144	41.49	5.711025
(c)	40.358	16.344	40.549	5.710975

Table 3: An example of the matrix elements

θ_1 and θ_3 represent the deviation of a phase advance between the second and the third cells and between the first and the second cells, respectively. Each unit is degree/ μ m.

$\partial\theta_1/\partial 2b_c$	0.44	$\partial\theta_1/\partial 2b_1$	0.07	$\partial\theta_1/\partial W$	0.07
$\partial\theta_3/\partial 2b_c$	-1.56	$\partial\theta_3/\partial 2b_1$	0.3	$\partial\theta_3/\partial W$	-0.08

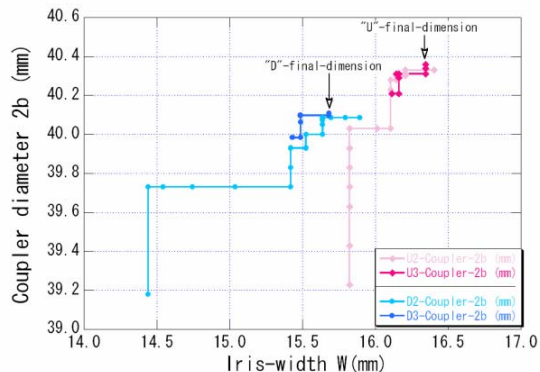


Figure 5: The history of the coupler dimension. The third couplers (U3-Coupler for input, D3-coupler for output) were used for CKK001.

ACKNOWLEDGMENT

The authors would like to thank to Mr. Iino Yousuke at Mitsubishi Heavy Industries, LTD. and also Mechanical Engineering Center of KEK for their cooperation in fabricating the accelerating section.

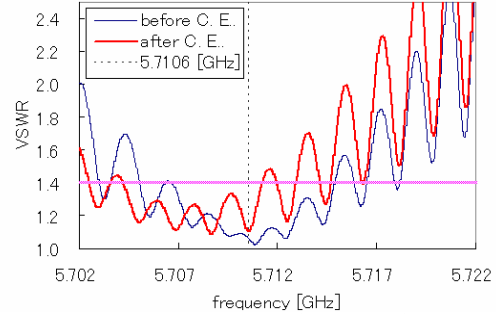


Figure 6: VSWR vs. Frequency before and after copper electroforming (abbreviated to C.E.).

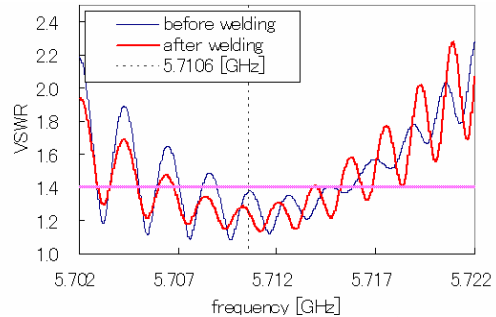


Figure 7: VSWR vs. Frequency before and after welding plungers.

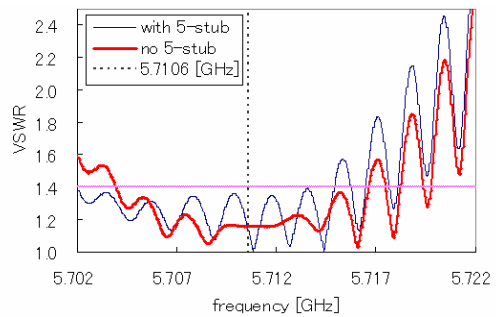


Figure 8: VSWR vs. Frequency before and after adjusting a 5-stub tuner. Target frequency is 5.7106GHz in the atmosphere.

REFERENCES

- [1] T. Kamitani et al., "Development of C-band Accelerating Section for SuperKEKB", Proceedings of LINAC 2004, Lübeck, Germany, Aug, 2004, pp663-665.
- [2] T. Kamitani et al., "R and D Status of C-Band Accelerating Section for SuperKEKB", this conference.
- [3] T. Sugimura, et al., "Development of C-band Accelerator Structure with Smooth Shape Couplers", this conference.
- [4] E. Westbrook, "Waveguides to the Disk-Loaded Accelerator Structure Operating in the $2\pi/3$ Mode", SLAC-TN-63-103.1963. Slac-TN-63-103, 1963.